Electronic supplementary information (ESI)

Immature dendritic cells navigate microscopic mazes to find tumor cells

Eujin Um, Jung Min Oh, Juhee Park, Taegeun Song, Tae-Eon Kim, Yongjun Choi, Changsik Shin, Diana Kolygina, Jae-Hyung Jeon, Bartosz A. Grzybowski,* and Yoon-Kyoung Cho*

Experimental Section (Continued)

Culture of breast cell lines

The β-MEKDD 116 cells were cultured in DMEM with 200 μg/mL G418, and EpH4-Ev cells in DMEM with 1.2 μg/mL puromycin. All media were supplemented with 5% FBS and 1% antibiotic-antimycotic solution. Both cells were maintained at 37 °C in a 5% CO_2 humidified incubator. All culture reagents were purchased from Gibco, and all cell lines were purchased from ATCC. When cancer cells were co-cultured with imDCs, the conditioned medium, RPMI 1640, supplemented with 5% FBS and 1% antibiotic-antimycotic solution, was used. To eliminate Gas6, EpH4-Ev and β-MEKDD 116 cells were pre-incubated with anti-Gas6 pAb (50 μg/mL; R&D systems), and as a control with anti-IgG pAb (50 μg/mL; Abcam), for 2 h at 37 °C and then washed in PBS (Gibco) prior to use.

Preparation of microchannels

The mold for microchannels was fabricated with SU-8 photoresist (MicroChem) using two-step photolithography. First, the photoresist (SU-8 2010) was spin-coated onto the silicon wafer to the height of 10 μm, which is the height for the migration tracks. Then, the first lithography was performed using a chrome mask containing different designs of microchannels. The second lithography was performed after spin-coating the same mold with photoresist (SU-8 2025) to the height of 50 μm, which formed the connecting channel between the reservoir and the migration tracks. The lengths of all straight migration channels were 380 μm.

Microchannels were fabricated by pouring a 10:1 mixture of polydimethylsiloxane (PDMS) prepolymer and the curing agent (Sylgard 184 Silicone Elastomer Kit; Dow Corning) onto the silicon wafer decorated with SU-8 molds. After curing the PDMS prepolymer in an oven at 65 °C for 2 h, the PDMS slab engraved with the channels was peeled off and holes were punched for the inlet and outlet reservoirs (3 mm in diameter). Circular glass coverslip (25 mm in diameter) and the prepared PDMS slabs were plasma-treated in a plasma cleaner (CUTE-1MPR, Femto Science Inc.) for 20 s at 100 W, and bonded to form the enclosed channels.

The entrance of all channels consisted of 5 μm-wide slits in order to block DCs from entering the microchannel due to flow at the initial stage of cell loading into the inlet. Also, the 5-μm slits created equal entrance dimensions for all 5, 10, and 50-μm wide tracks, creating the same conditions for cell entrance. Pillars were placed near the outlets and were spaced 2-3 μm apart, in order to block cancer cells from entering the migration tracks.

Transwell migration assay

BMDCs (1×10^5 cells) were placed in 5-μm pore insert of a 24-well Transwell plates (Corning Costar). The lower chamber was filled with the conditioned medium from either EpH4-Ev or β-MEKDD 116 cells cultured for 18 h in complete medium (RPMI 1640), or blank medium as control. DCs were incubated for 6 h at 37 °C in 5% CO_2. The imDCs that migrated to the lower chamber and those that remained on the insert were collected separately, and analyzed by flow cytometry (FACSVerse, BD Biosciences) for the expression of CD86, CD80, and CD40. Anti-CD11c APC and anti-CD86 PE antibodies were purchased from BD-Biosciences, and anti-CD80 FITC and anti-CD40 PE antibodies were purchased from Thermo Fisher Scientific. All experiments were performed in triplicate for

each condition and the FACS data was analyzed using FlowJo (Tree Star) software.

Gene expression of imDCs

The total RNA was extracted from imDCs using the PureLink RNA mini kit (Thermofisher). The quantity and the quality of RNA were measured by the 11 Spectrophotometer (DeNovix Inc.) and Fragment Analyzer (Advanced Analytical Technologies). RNA samples were hybridized using nCounter GX mouse immunology kit V1 (561 genes; NanoString Technologies). Total RNA (100 ng) was subsequently incubated overnight at 65 °C in nCounter Reporter CodeSet, Capture ProbeSet, and hybridization buffer. Following hybridization, excess probes were immediately removed by the nCounter PrepStation, and the samples were analyzed on an nCounter Digital Analyzer. mRNA data analysis was performed using the nSolver software analysis. The mRNA profiling data was normalized using housekeeping genes. All samples were processed in biological duplicates.

Cytokine antibody array and quantification of Gas6

Assay on mouse cytokine array (Raybiotech, AAM-CYT-2000, detecting 144 proteins) was performed according to the manufacturer's instructions, with cell-conditioned media from EpH4-Ev and β-MEKDD 116 cells, collected after 18 h of culture. The scanned result of cytokine expression was analyzed using ImageJ software and normalized using internal positive controls. Concentrations of soluble Gas6 in cell supernatants from EpH4-Ev and β-MEKDD 116 cells were quantified using a mouse GAS6 ELISA kit (Raybiotech) according to the recommended protocol, after culturing 2.7×10^5 cells per well in 24 well plate for 18 h.

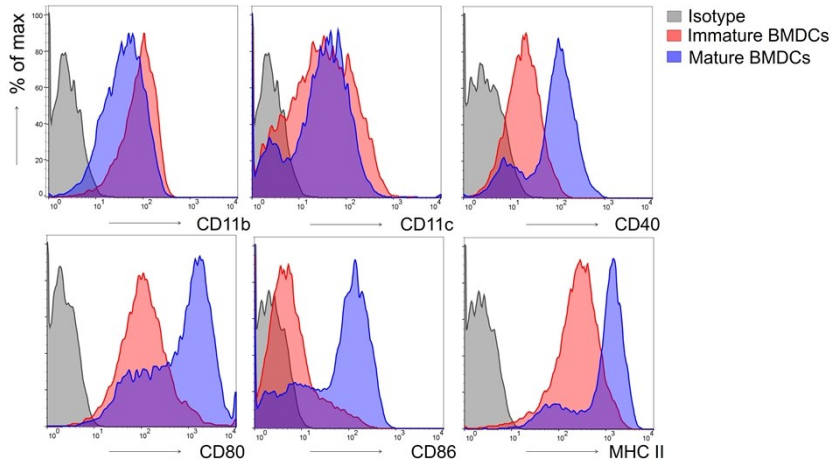

Fig. S1 Expression of maturation markers on DCs. Flow cytometry analysis of maturation markers on immature DCs (imDC) and mature DCs (mDC). The red and blue distributions correspond to staining of imDCs and mDCs, respectively. The gray distributions are for isotype control staining. The results shown are from one experiment and are representative to data from more than five independent experiments we carried out.

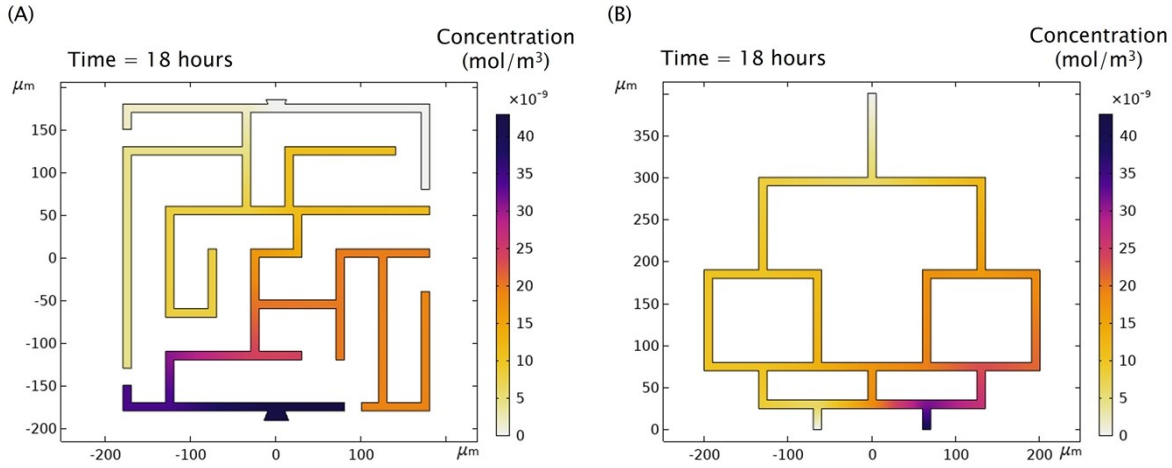

Fig. S2 Simulation of the concentration gradient of representative chemoattractant with diffusivity 5e-11 [m^2/s] using COMSOL program. Time-dependent diffusion equation was solved with FEM (finite element method) with linear shape function, spatial discretization scheme, and time stepping method of 2nd-order Backward Differentiation Formula (BDF). The images capture the concentration gradient after 18 hours, when the maximum concentration in the outlet reaches 4.3×10^{-8} mol/m^3 in (A) a complex maze (triangular mesh with 9335 elements) and (B) a bifurcating channel of two outlets (triangular mesh with 6612 elements).

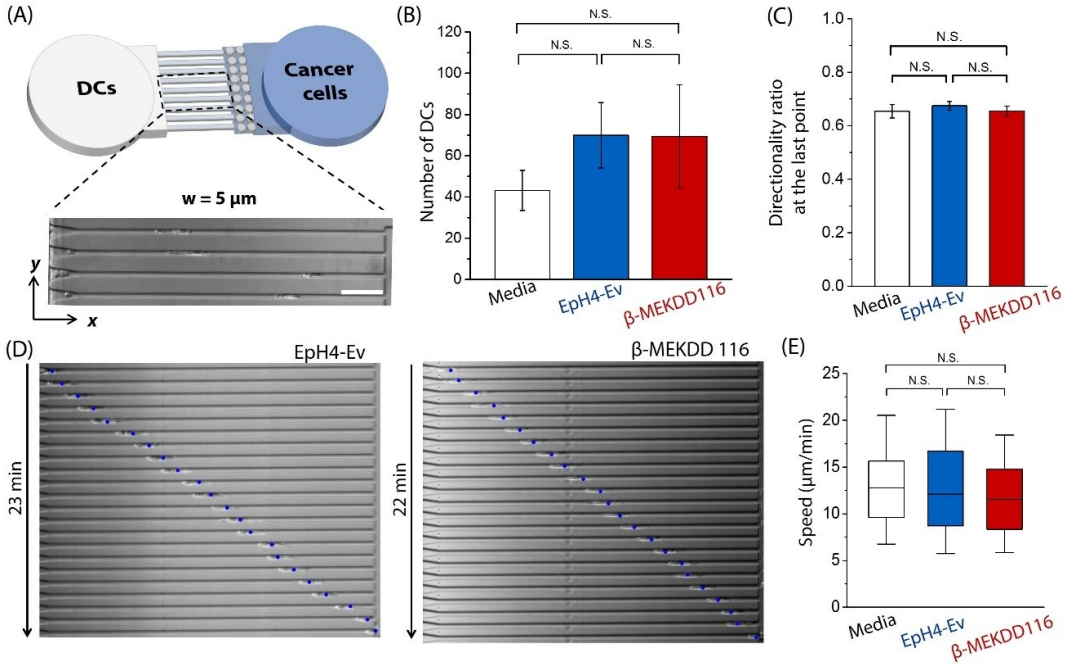

Fig. S3 Migration of imDCs in 5-µm-wide channels. (A) Schematic image of the microchannel array of 5-µm width, connecting the inlet for imDCs and the outlet. Microscope image captures imDCs migrating inside the microchannels. Scale bar = 50 µm. (B-C) Bar graphs showing (B) the average number of imDCs that exited the channels towards the outlet per device (n = 6 independent devices; each device containing 32 channels), and (C) the average directionality ratio at the last point of tracking. Results are expressed as mean ± s.e.m. (D) imDC migrating in the presence of EpH4-Ev (left), and β-MEKDD 116 (right), both exhibiting directionality ratio at the last point, 1. (E) Average speed of imDCs represented as box and whisker (10-90 percentile) plots. A Mann-Whitney test was applied for all statistical analyses. *P < 0.05, **P < 0.01, ***P < 0.001, and ****P < 0.0001.

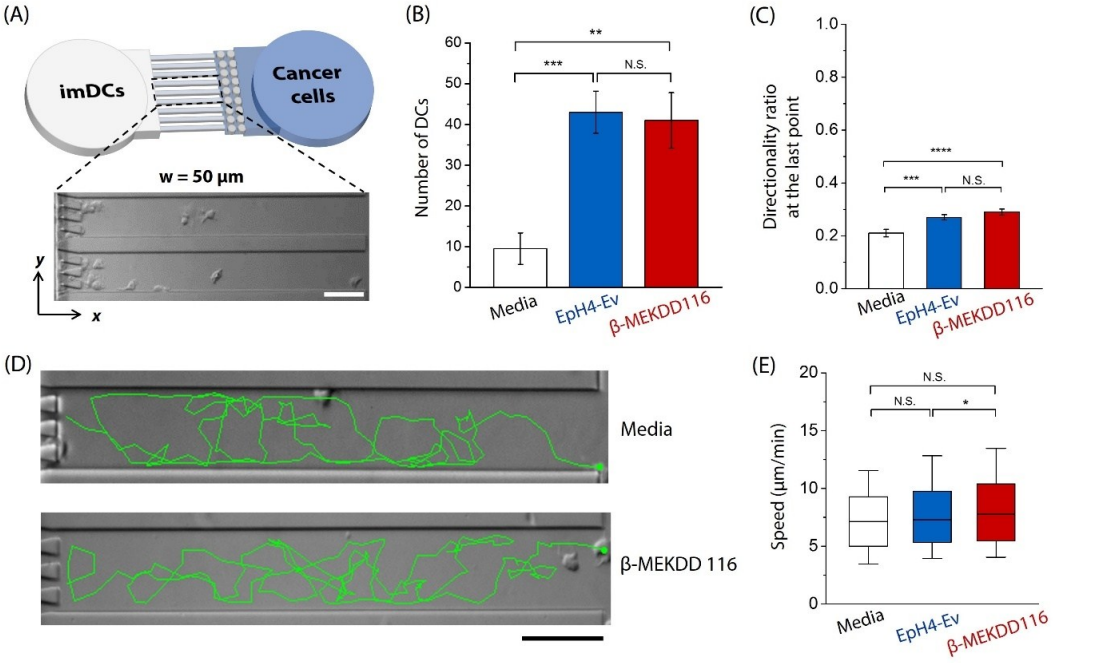

Fig. S4 Migration of imDCs in 50-µm-wide channels. (A) Schematic image of the microchannel array of 50-µm width, connecting the inlet for imDCs and the outlet. Microscope image captures imDCs migrating inside the microchannels. (B-C) Bar graphs showing (B) the average number of imDCs that exited the channels towards the outlet per device (n = 6 independent devices; each device containing 10 channels), and (C) the average directionality ratio at the last point of tracking. Results are expressed as mean ± s.e.m. (D) Representative imDCs migrating in the presence of blank medium (above) and β-MEKDD 116 (below), both showing complex trajectories. (E) Average speed of imDCs represented as box and whisker (10-90 percentile) plots. A Mann-Whitney test was applied for all statistical analyses. **P* < 0.05, ***P* < 0.01, ****P* < 0.001, and *****P* < 0.0001. Scale bars = 50 µm.

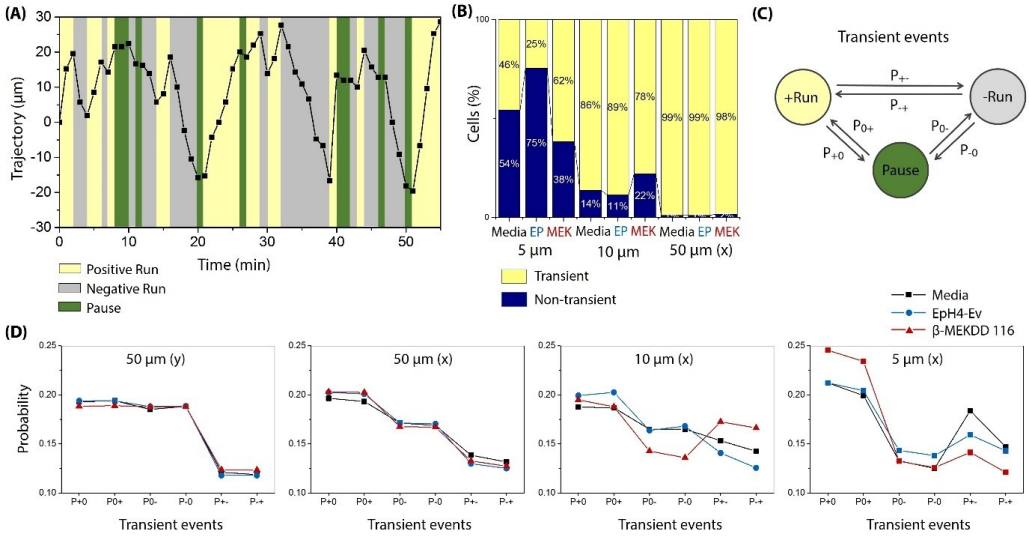

Fig. S5 Additional analyses of imDC trajectories. (A) Plot of a typical imDC trajectory in 10-μm confinement (in x-direction) over time, classified as three types of transient events: positive runs (direction towards the outlet), negative runs (direction towards the opposite of outlet), and pauses. The pause event was defined if the cells did not move more than 3 μm between frames of 1 minute. If imDCs continued their positive run throughout the whole observation time without changing the events, we called them non-transient cells. (B) Percentages of transient cells and non-transient cells in each condition of confinement, among all imDCs migrating towards medium, EpH4-Ev (EP), and β-MEKDD 116 cells (MEK). The percentages of non-transient cells were higher in tighter confinements. (C) Change of the events between positive run (+Run), negative run (-Run), and Pause in transient cells renders six probabilities, P+0 and P0+ (probabilities to change between Pause and +Run), P0- and P-0 (probabilities to change between Pause and -Run), and P+- and P-+ (probabilities to change between +Run and -Run). **(D)** Probability distribution of the six event changes in migrating imDCs, in each confinement (width of the confinement and direction of movement is as mentioned at the top of each graph). We found that among transient cells, the probability of changing the event from +Run to –Run (P+-) or –Run to +Run (P-+), without pause in-between, was most manifest in narrower, 10- and 5-μm channels of, and less likely to occur in 50-μm channels.

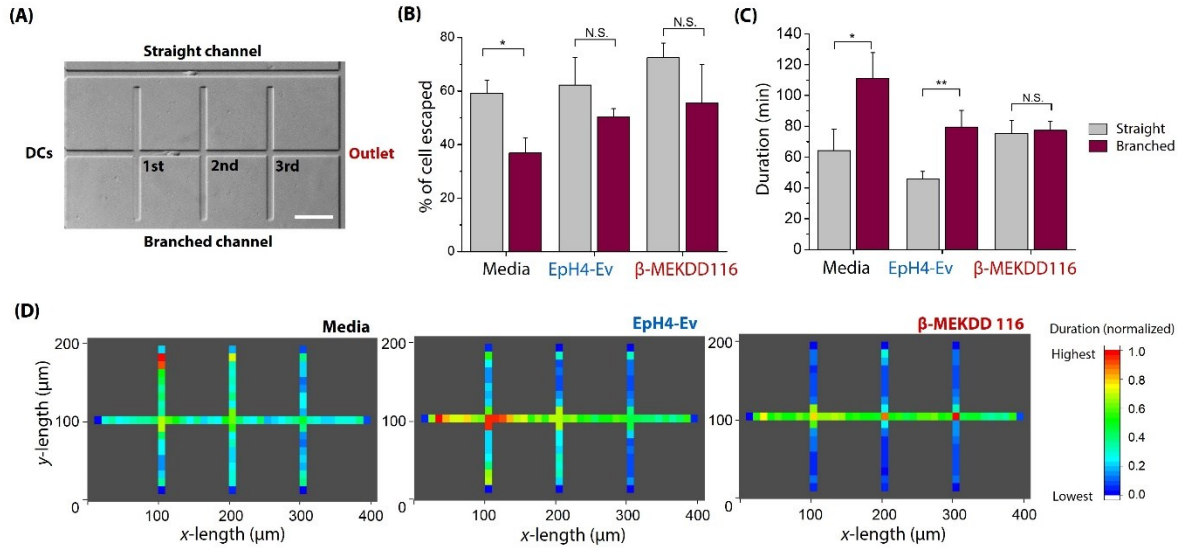

Fig. S6 Migration of imDCs in branched channels. (A) Microscopic image of a channel with three perpendicular branches placed next to the straight channel of the same width and height for comparison. Scale bar = 50 μm. (B) Percentages of imDCs escaping from the branched channel, compared to the straight channel of the same width and height. (C) The exit time of the escaped imDCs (duration) from the branched channel, in comparison with the straight channel of the same width and height. (D) Color maps showing the dwell time of imDCs at each position within the channels (accumulated time data of all visiting cells, normalized to 0-1).

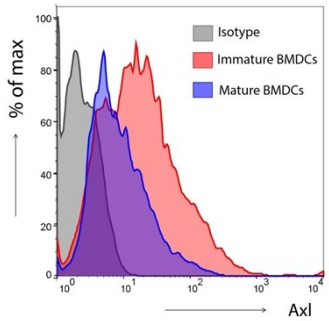

Fig S7 Flow cytometry analysis of the Axl marker on immature DCs and mature DCs. The red and blue distributions correspond to staining of imDCs and mDCs, respectively. The gray distribution is for isotype control staining. The results shown here are from one experiment, which are representative data of more than five independent experiments we carried out.

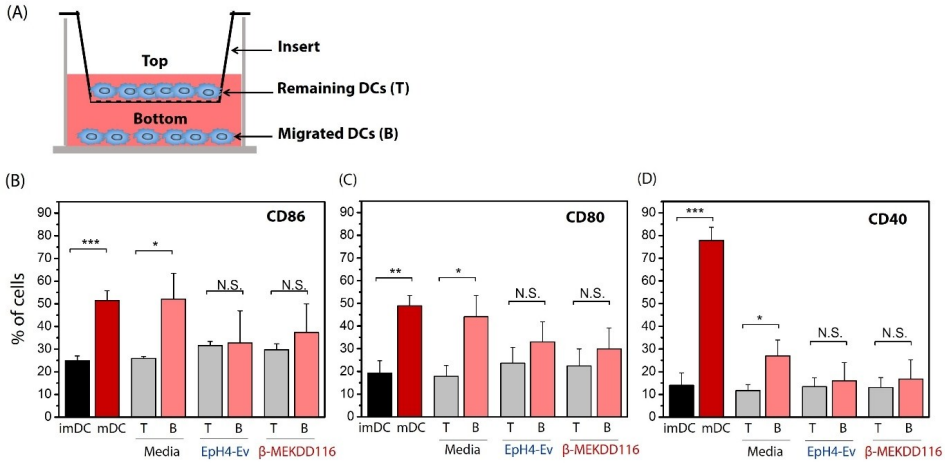

Fig. S8 Summary of results from Transwell migration assay. (A) Schematic of the Transwell migration assay of DCs in cell-conditioned medium. Comparison of the percentages of DCs expressing maturation markers, (B) CD86 (C) CD80 and (D) CD40, among the DCs that migrated to the bottom (pale red color, B) and the remaining stationary DCs at the top (gray color, T).

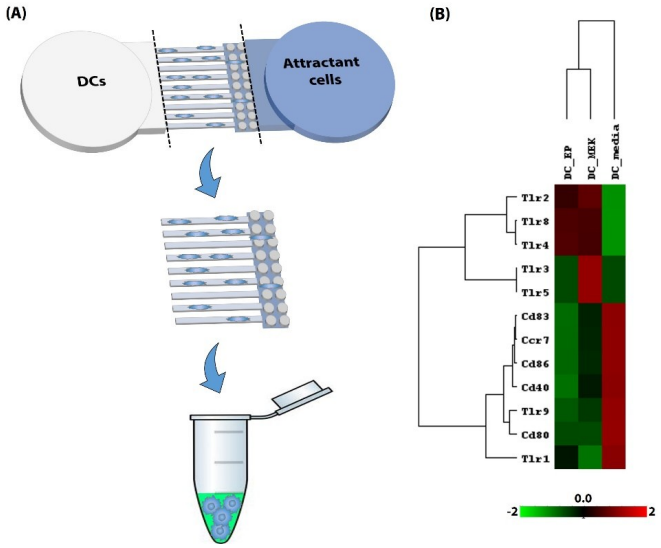

Fig. S9 Gene expression profile of the migrated DCs from a 10-µm microchannel. (A) A scheme depicting collection of the migrating DCs. Only DCs in the region of the migration channels and the pillars were collected from the device after the inlet and outlet reservoirs had been cut out. (B) Heatmap of gene expressions of DC maturation markers and TLR-related genes, showing the difference between DCs migrating towards EpH4-Ev, β-MEKDD 116 cell lines and control media.

Table S1. Signal intensities (in arbitrary unit) from the cytokine array profiling using cultured media from the EpH4-Ev and β-MEKDD116 cells, organized in the order from the highest to the lowest relative expression ratio (β-MEKDD116/EpH4-Ev)

	Expression level		Relative ratio
Cytokine	**EpH4-Ev**	**β-MEKDD 116**	**β-MEKDD 116/ EpH4-Ev**
Gas 6	88.4	1188.2	13.5
Pro MMP-9	269.6	1062.7	3.9
Pentraxin-3	41.5	160.8	3.9
Axl	79.9	180.8	2.3
HGF	25.5	50.7	2.0
JAM-A (CD321)	472.8	893.0	1.9
Neprilysin	48.5	89.6	1.9
BLC (CXCL1 3)	63.1	113.9	1.8
CRG-2	60.9	108.2	1.8
GM-CSF	154.6	274.1	1.8
Gas 1	41.0	68.5	1.7
CD30L	80.6	133.8	1.7
CCL24	74.6	121.0	1.6
IL-1 alpha	344.6	555.6	1.6
Il-2 R alpha	21.0	33.2	1.6
IL-1 RA	58.7	92.4	1.6
AR	119.1	178.8	1.5
Decorin	43.0	63.1	1.5
IL-9	50.0	73.4	1.5
CD40L	83.9	123.0	1.5
Prolactin	22.9	32.9	1.4
Leptin R	259.6	370.4	1.4
IL-3 R beta	164.4	228.5	1.4
MCP-1 (CCL2)	1064.0	1456.4	1.4
IGF-2	164.3	224.3	1.4
TCA-3/CCL1	734.4	989.9	1.4
IL-12 p40/p70	75.0	100.6	1.3

IL-13	76.5	102.5	1.3
P-Selectin	546.3	725.4	1.3
IL-21	64.9	85.7	1.3
RANTES (CCL5)	1410.9	1830.8	1.3
CXCL4	825.8	1066.6	1.3
Galectin-1	2523.3	3222.9	1.3
IL-6R	131.1	164.4	1.3
Ltn (XCL1)	127.1	159.2	1.3
CTACK	1056.6	1306.1	1.2
TREM-1	152.1	181.6	1.2
ALK-1	128.6	153.5	1.2
IL-17F	41.9	49.1	1.2
IL-4	818.1	932.1	1.1
IGFBP-1	1284.0	1461.7	1.1
IL-1 1	659.2	742.6	1.1
MCP-5	249.5	276.6	1.1
ICAM-1 (CD54)	1425.9	1568.5	1.1
Granzyme B	84.9	92.6	1.1
IL-1 R4 (ST2)	1115.3	1200.1	1.1
MIP-1 gamma	2721.3	2923.6	1.1
IGF-1	857.4	909.7	1.1
Lungkine (CXCL15)	947.5	996.2	1.1
IL-28A	1492.7	1567.0	1.1
CXCL16	3311.5	3462.2	1.1
TPO	169.7	176.1	1.0
IL-12p70	1112.3	1132.0	1.0
CX2CL1	153.8	155.9	1.0
MIP-2 beta (CCL19)	87.2	88.0	1.0
M-CSF	856.4	853.6	1.0
CD36 (SR-B3)	84.7	83.8	1.0
TIMP-1	987.5	937.3	1.0

CCL21	1245.5	1179.8	1.0
IGFBP-3	1768.3	1664.4	0.9
TWEAK R (TNFRSF12)	3324.0	3086.0	0.9
IL-17B	139.1	126.1	0.9
OPN (SPP1)	5850.0	5281.1	0.9
LIX	5458.2	4821.2	0.9
MMP-3	3686.8	3102.8	0.8
DKK-1	279.5	232.1	0.8
bFGF	185.8	153.1	0.8
MIP-2	2088.0	1710.7	0.8
MHG-E8	86.6	70.6	0.8
KC (CXCL1)	1272.7	1022.4	0.8
Epiregulin	59.9	41.4	0.7
TNFRSF1A	2023.1	1360.1	0.7
GCSF	5486.6	3526.5	0.6
TNFRSF1B	2060.1	1299.6	0.6
E-Cadherin	5637.8	3275.2	0.6
MIP-3 alpha (CCL20)	1251.2	655.9	0.5
IGFBP-6	1046.5	479.6	0.5
VEGF-A	1240.7	497.4	0.4
TCK-1 (CXCL7)	6765.5	2284.9	0.3

List of Movies

All videos play at × 600 speed.

1. ESI Movie 1 – ImDCs in a complex maze, moving towards β-MEKDD 116 cells in the outlet

2. ESI Movie 2 – ImDCs in the bifurcating channels leading to two outlets, left (EpH4-Ev cells) and right (β-MEKDD 116 cells)

3. ESI Movie 3 – ImDCs in 10-µm-wide channel moving towards (A) medium, (B) EpH4-Ev, and (C) β-MEKDD 116 cells in the outlet

4. ESI Movie 4 – ImDCs in 5-µm-wide channel moving towards (A) medium, (B) EpH4-Ev, and (C) β-MEKDD 116 cells in the outlet

5. ESI Movie 5 – ImDCs in 50-µm-wide channel moving towards (A) medium, (B) EpH4-Ev, and (C) β-MEKDD 116 cells in the outlet

6. ESI Movie 6 – ImDCs in the branched channel moving towards (A) medium, (B) EpH4-Ev, and (C) β-MEKDD 116 cells in the outlet